

Helical Structure of the Cardiac Ventricular Anatomy Assessed by Diffusion Tensor Magnetic Resonance Imaging Multi-Resolution Tractography

Ferran Poveda^{a,b}, Debora Gil^{a,b}, Enric Martí^b, Albert Andaluz^a, Manel Ballester^c,
Francesc Carreras^d

^aComputer Vision Center, Universitat Autònoma de Barcelona, Spain

^bComputer Science Department, Universitat Autònoma de Barcelona, Spain

^cDepartment of Medicine, Universitat de Lleida, Lleida, Spain

^dCardiac Imaging Unit, Hospital de la Santa Creu i Sant Pau, Barcelona, Spain

Abstract

Deep understanding of myocardial structure linking morphology and function of the heart would unravel crucial knowledge for medical and surgical clinical procedures and studies. Several conceptual models of myocardial fiber organization have been proposed but the lack of an automatic and objective methodology prevented an agreement. We sought to deepen in this knowledge through advanced computer graphic representations of the myocardial fiber architecture by diffusion tensor magnetic resonance imaging (DT-MRI). We performed automatic tractography reconstruction of unsegmented DT-MRI canine heart datasets coming from the public database of the Johns Hopkins University. Full scale tractographies have been build with 200 seeds and are composed by streamlines computed on the vectorial field of primary eigenvectors given at the diffusion tensor volumes. Also, we introduced a novel multi-scale visualization technique in order to obtain a simplified tractography. This methodology allowed keeping the main geometric features of the fiber tracts, making easier to decipher the main properties of the architectural organization of the heart. On the analysis of the output from our tractographic representations we found exact correlation with low-level details of myocardial architecture, but also with the more abstract conceptualization of a continuous helical ventricular myocardial fiber array. Objective analysis of myocardial architecture by an automated method, including the entire myocardium and using several 3D levels of complexity, reveals a continuous helical myocardial fiber arrangement of both right and left ventricles, supporting the anatomical model of the helical ventricular myocardial band described by F. Torrent-Guasp.

Keywords: heart, diffusion magnetic resonance imaging, diffusion tractography, helical heart, myocardial ventricular band

1. Introduction

It is widely accepted that the myocardial fiber architecture plays a critical role in many functional aspects of the heart such as electrical propagation [1, 2] or ventricular contraction [3, 4]. It is also accepted that myocardium, as well as its fibers, may undergo architectural alterations in many heart diseases [5, 6] leading to inefficient heart function. However, there is a lack of consensus about the exact distribution of the myocardial fibers and their spatial arrangement that constitutes the gross (left and right ventricles) myocardial structure. Deep understanding of the precise cardiac architecture [7] and its relation with ventricular function [8] would benefit several clinical procedures such as surgery planning in left ventricular reconstructive surgery or resynchronization therapies [9, 10].

Researchers have proposed several conceptual models (at least 7) [11] trying to accurately describe the architecture of the heart either from dissection or histological procedures. Two of the most controversial conceptual models approaches are the cardiac mesh model proposed by Anderson [12, 13] and the Helical Ventricular Myocardial Band (HVMB) proposed by TorrentGuasp [14, 15]. The cardiac mesh model proposes that the myocytes are arranged longitudinally and radially, changing its angulations along with myocardial depth and binding this architectural disposition to a functional one [16]. On the other side, the HVMB model states that the ventricular myocardium is a continuous anatomical helical layout of myocardial fibers, linking the ventricular anatomy to the well described cardiac torsion mechanics [17].

The problem in the studies of ventricular models is that unlike skeletal muscles, myocardial tissue is locally arranged in a discrete mesh of branching myocytes [18]. This entangled structure is prone to hinder or even mislead the interpretation of “tracts” which define the muscular structure of the myocardium. Some researchers argue that the interpretation of such “tracts” depends on the dissection procedures [12].

During the last decade, a new modality of magnetic resonance imaging, diffusion tensor magnetic resonance imaging (DT-MRI) has enabled computational validation of the muscular structure of the heart. This technique provides a discrete measurement of the three-dimensional (3D) arrangement of myocytes [19] by the observation of local anisotropic diffusion of water molecules in biological tissues [20]. DT-MRI has been established as the reference imaging modality for the measurement of the whole cardiac architecture with acceptable resolution ($300\ \mu\text{m} \times 300\ \mu\text{m} \times 1000\ \mu\text{m}$) compared to size of myocytes ($50 - 100\ \mu\text{m}$ long and $10 - 20\ \mu\text{m}$ thick). Indeed, DT-MRI provides a summary of the microscopic mesh enhancing the preferred pathway of the connected myocytes, which constitutes the concept of myocardial fiber.

In the present work advanced computer graphics techniques were used to provide an objective and comprehensive description of the myocardial fiber architecture, as previously communicated [21], and we introduce a multiresolution tractographic approach to provide a simplified and comprehensive understanding of the heart architecture.

2. Methods

Datasets used in this study come from the public database of the Johns Hopkins University [22]. These datasets were obtained from 4 normal canine hearts. Each heart

was placed in an acrylic container filled with Fomblin, a perfluoropolyether (Ausimon, Thorofare, NJ). Fomblin has a low dielectric effect and minimal MR signal thereby increasing contrast and eliminating unwanted susceptibility artifacts near the boundaries of the heart. The long axis of the hearts was aligned with the z-axis of the scanner.

Images were acquired with a 4-element knee phased array coil on a 1.5 T GE CV/I MRI Scanner (GE, Medical System, Wausheka, WI) using an enhanced gradient system with 40 mT/m maximum gradient amplitude and a 150 T/m/s slew rate. Hearts were placed in the center of the coil and a 3D fast spin echo sequence was used to acquire diffusion images with a minimum of sixteen non-collinear gradient directions and a maximum b-value of 1500 s/mm². The size of each voxel was about 312.5 μm x 312.5 μm x 800 μm . Resolution resulting from a zero padding in fourier space to adapt original image size of 192x192 to 256x256. The final dataset was arranged in about 256 x 256 x 108 arrays (depending on the scanned heart) and contains two kinds of data: geometry/scalar data and diffusion tensor data. For diffusion tensor data, each voxel in the array consisted of 3 eigenvalues and 3 eigenvectors. The size of each voxel was about 312.5 μm x 312.5 μm x 800 μm .

Full scale tractographies presented in this study have been built with 200 seeds. These seeds have been randomly chosen over the entire anatomy only taking out a very small range of points related to the lowest eigenvalues that are likely to be bad starting points for the reconstruction. The strategy for the seed selection in the reconstructions of lower resolution in the scale-space has been to scale proportionally these values to the downscaling magnitude.

3. Key Points for Ventricular Tractography Reconstruction

3.1. Data completeness

It is undisputed that the basal ring is crucial to fully understand heart anatomy and function. However, in some publications [23, 24, 25] the myocardial volume is cut just below the mitral valve to avoid noisy tractography in the auricular cavities. Given that such plane cut discards, the basal ring reconstructions are not complete for a reliable interpretation of the cardiac architecture.

3.2. DT-MRI Vector field orientation

Tractography is a technique inherited from the study of fluids. In this field orientation of vector fields stands for fluid stream directions and, thus, reconstructions present no ambiguity. However, in the case of anatomical structures DT-MRI vector fields have an orientation that does not correspond to any physiological property. For a successful tractography reconstruction, DT-MRI vector fields should be reoriented. The few existing approaches are based on either local properties of the flux or parametric models of the heart. By their local nature, local approaches[24] might introduce suboptimal fibers not consistent with the global structure. Although parametric models of the ventricles [26, 27] provide a good solution to solve fiber orientation, because of their complexity, they are usually restricted to the left ventricle. We propose a geometrical organization coherent to gross heart anatomy.

3.3. Visualization

Comprehensive visualization of fiber tracts should involve a proper assignment of colors providing information about the orientation of the myocardial fibers. Often color maps are defined using a global coordinate system which might mislead the global structure. In order to properly encode the anatomical structure, color maps based on local information should be considered.

3.4. Heart architecture interpretation

Fully detailed tractographic reconstructions fit perfectly to make low level descriptions, but might fail on a higher level of analysis as a result of their complexity. In order to obtain more comprehensive descriptions of global myocardial structure we propose the use of a multiresolution approach applied to the standard tractographic algorithms. This may help to generate simpler visualizations which in turn may help to better understand the detailed myocardial architecture.

4. Fullscale Tractography

Heart tractography is seen as a reconstruction composed by several streamlines [28] (also known as fiber tracks on this field). The main property that clearly defines a streamline is that it is a curve tangential to the vector field at any point of such curve.

In this work, tractographies will be composed by streamlines computed on the vectorial field of primary eigenvectors given at the diffusion tensor volumes. We computed those streamlines using a fifth order Runge-Kutta-Fehlbert [29] integration method

4.1. Data completeness

In order to get complete reconstructions of the myocardial anatomy we have considered the whole DT-MRI volumes including the atrial cavities and the basal ring. Noise on the streamline reconstruction is mainly caused by thin atrial tissue which introduces significant clutter on the visualization. In order to minimize such artifact, our streamlining method stops integration of streams with large Runge-Kutta estimated reconstruction error.

4.2. DT-MRI Vector field orientation

Tractography is a graphical representation inherited from fluid mechanics where both direction and orientation of the vector fields are a meaningful part of the represented information. However, on DT-MRI data vectors can be considered bidirectional seeing that the water diffusion represented by this eigenvector occurs in one dimension but it does on the two possible orientations at the same time. Sometimes the datasets will have a nearly organized structure, but we can also get opposed orientations (Fig. 1a) at some points of the vectorial field that hinder its reconstruction.

We apply a geometrical reorganization of the vector field using local coordinate systems coherent to ventricular anatomy and fluid mechanics. Ventricular anatomy can be described by means of a longitudinal axis and angular coordinates with respect to this axis on axial cuts. In order to properly reorient both ventricles, our longitudinal axis has been set across the left ventricle, near the septum, ensuring that it never crosses

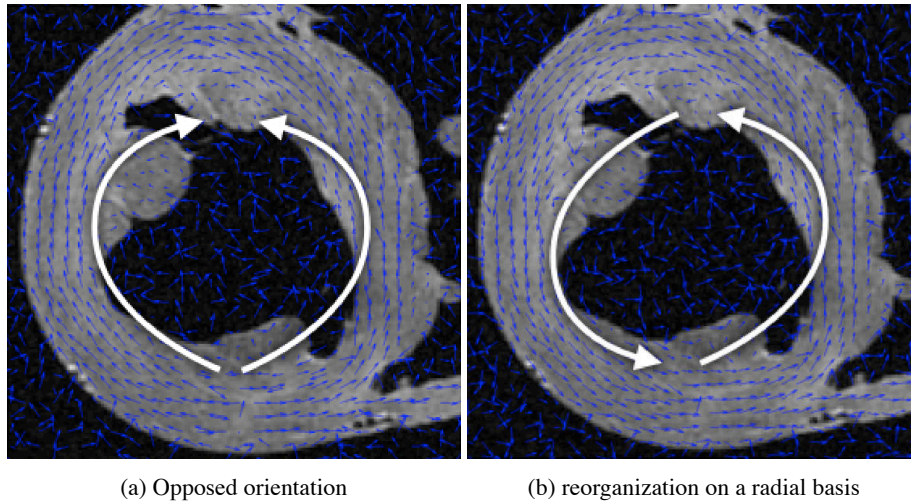


Figure 1: Orientation of the vectorial field datasets.

any myocardial wall. In order to make valid the vector field for streamlining this axis should define for each axial cut a center of rotation. Therefore at every axial cut of the DT-MRI we reorganize vector orientations on a stream-like fashion (Fig. 1b) around the point where the coordinate axis intersects the same axial cut. This implementation allows fast reorientation avoiding any smoothing of the vectorial field.

4.3. Anatomical-based fiber colouring

The previous reorientation allows colouring techniques based on axial and longitudinal angulations of fibers that may help in the interpretation of the tractographic models. Different color mappings coherent to these directions allow highlighting different features of the fiber architecture adding valuable information of existent muscular layers. Color maps tuned on longitudinal angulation are the ones that convey more valuable information about muscular layers. Figures 2 and 3 show two different views of the longitudinal color map of the reconstructed fibers.

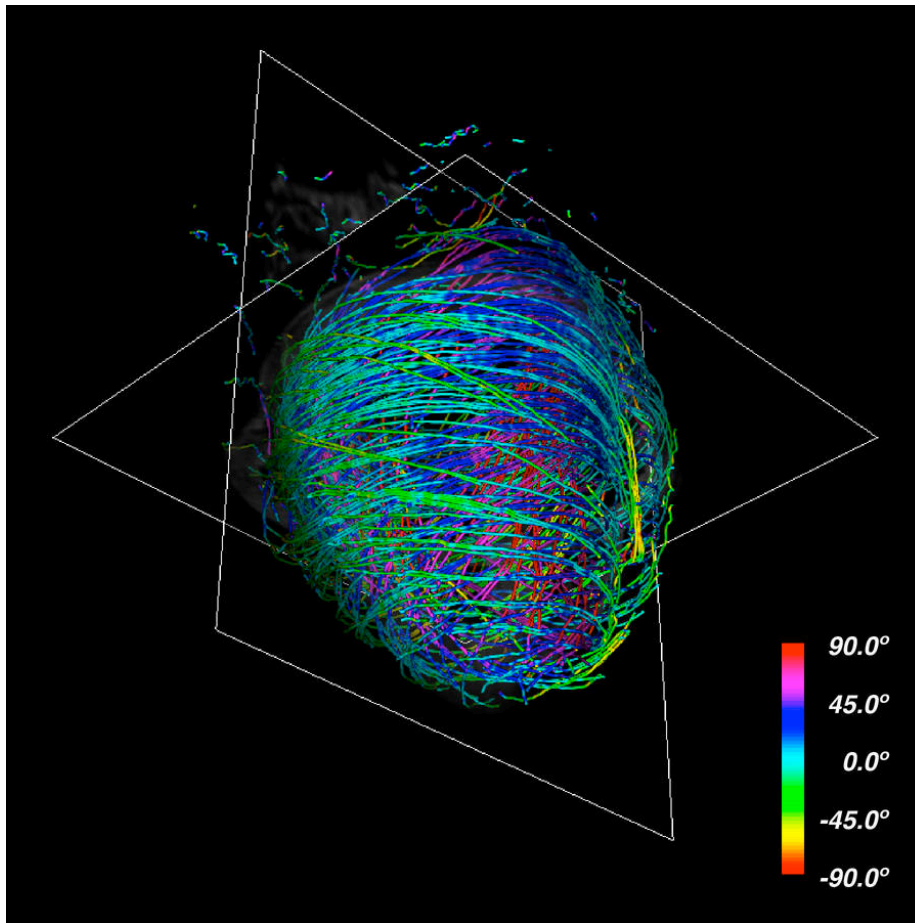


Figure 2: Color map of the reconstructed fibers. Full scale tractography reconstruction with near 350 seeds. Represented on a full-color scheme determining orientations of the fibers.

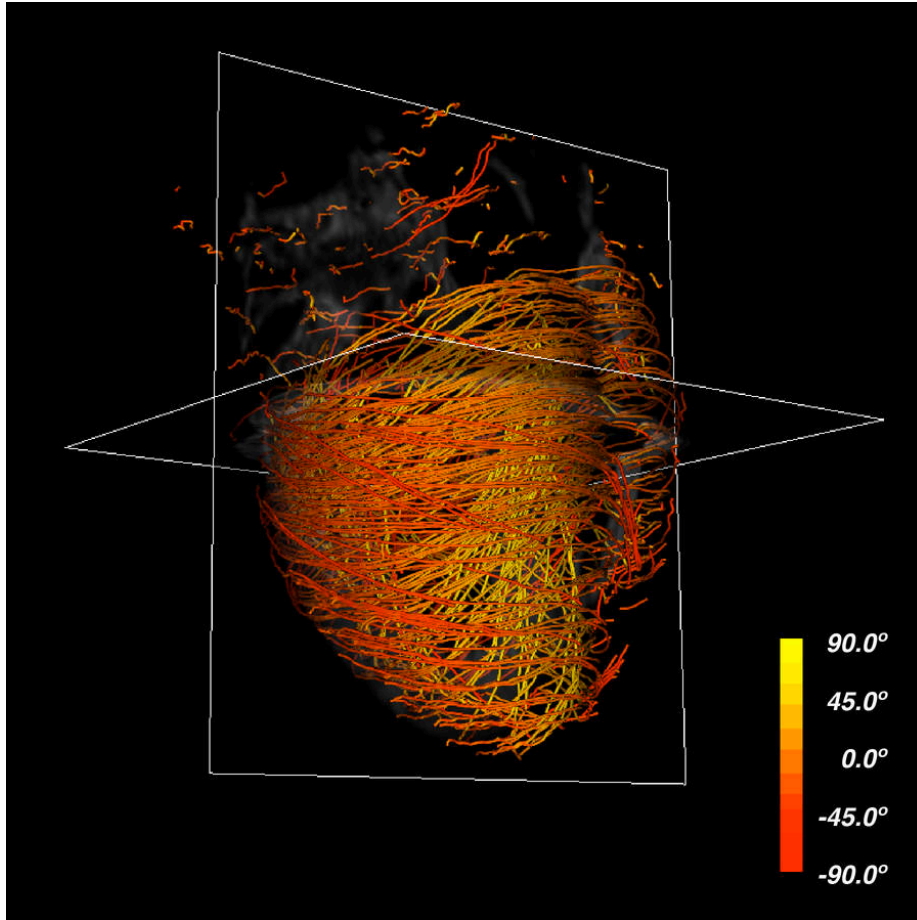


Figure 3: Color map of the reconstructed fibers. Two-color scheme set raise the difference between ascending and descending fibers.

5. Multi-Resolution Tractography

The representation of a fully detailed tractography has been the state of the art methodology to work out the comprehension of the heart. On this task, tractographic models have achieved interesting results but have also demonstrated weakness not helping to clarify a widely accepted unique myocardial anatomy description.

Intuitively, on a real world context, when an observer tries to make a gross analysis he can step away a few meters from the object of analysis and get a more contextual view. We will extrapolate this everyday behaviour to our problem.

In order to resolve this in a computer graphic representation it is common to use multiresolution models which try to find solutions to build different models of the same data with different levels of detail but without a loss of fidelity. It is usually applied to texture mapping and it is known as mipmapping [30] based on the well known pyramid representation [31]. This technique applies a Gaussian filtering and later an exponential reduction via a subsampling of the full-scale texture. Reduced textures are somehow “summaries” of the original texture and would be used to represent this texture at different scales. These “summaries” are statistically complete in such a way the Gaussian smoothing keeps the contextual information before applying downsampling. The use of these downsampled images is also common in other fields like in computer vision where this operation can be seen as a computation on the scale space.

This technique can be applied to the DT-MRI dataset in order to simplify its complexity. By downscaling two orders of magnitude of the original datasets and applying our streamlining, we get the simplified tractography shown in 4. Comparing to the full scale tractography shown in figure 2 it is easy to notice that the simplified one keeps the main geometric features of fibers. Therefore it allows an easier identification of global morphological tendencies.

6. Results

Our simplified tractographic reconstruction method (Fig. 4) keeps the main geometric features of fibers allowing an easier identification of global tendencies. In turn, these tendencies show a manifest continuous helical structure of the ventricular myocardium. We sought to compare the results of the tractography with the anatomy of the helical ventricular myocardial band (HVMB) described by F. Torrent-Guasp [16].

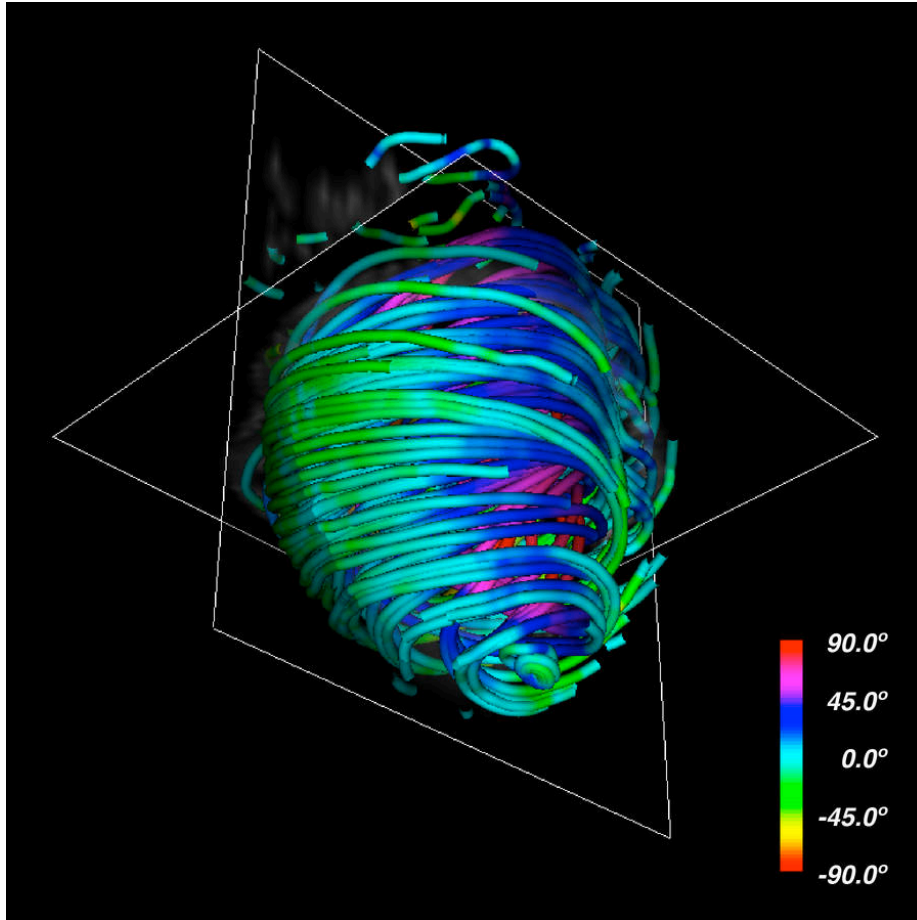


Figure 4: Simplified tractography. A simplified tractography is obtained by downscaling twoorders of magnitude of the original datasets.

HVMB describes a longitudinal arrangement of ventricular myocardial fibers forming a unique functional muscular band (Fig. 5) starting at the pulmonary artery (PA) and finishing at the aorta (Ao). This muscle wraps the left ventricle and part of the right ventricle (right and left segments) connecting to an helicoidal structure starting at the basal ring going inside the left ventricle towards the apex and returning to connect with the aorta (descending and ascending segments) wrapping with this turn the entire anatomy of the heart.

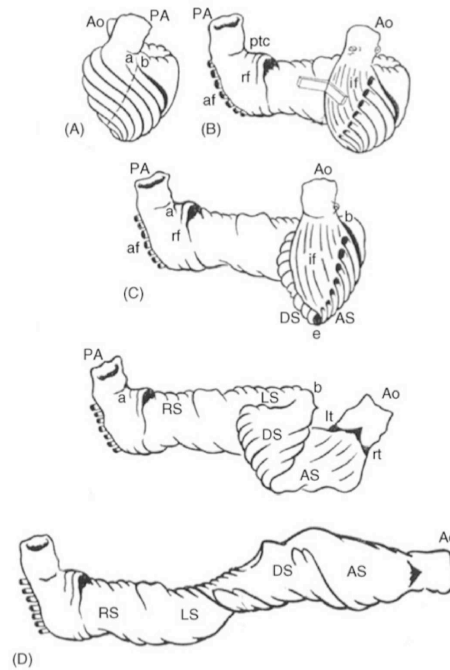


Figure 5: Ventricular myocardial band. Schematic presentation of the ventricular myocardial band dissection. Ao, aorta; PA, pulmonary artery; ptc, pulmonary-tricuspid cord; af, aberrant fibers; rf, right septal fibers; if, intra-septal fibers; AS ascending segment; DS, descending segment; LS left segment; RS right segment; lt, left trigone; rt, right trigone.

6.1. Fullscale Tractography

For the purpose of comparing tractographic results with the band model, step by step tractographic reconstructions were compared with the myocardial fiber tracts depicted at the Torrent-Guasp's rubber-silicone mould of the HVMB [32] (Figs. 6,7,8,9).

6.1.1. Right Segment

starting the analysis on the right segment a clear pattern is observed where the reconstructed tracts on the epicardium are orientated towards the basal ring. These tracts loop at the basal ring towards the endocardium describing which looks like as a simple folding (Fig. 6).

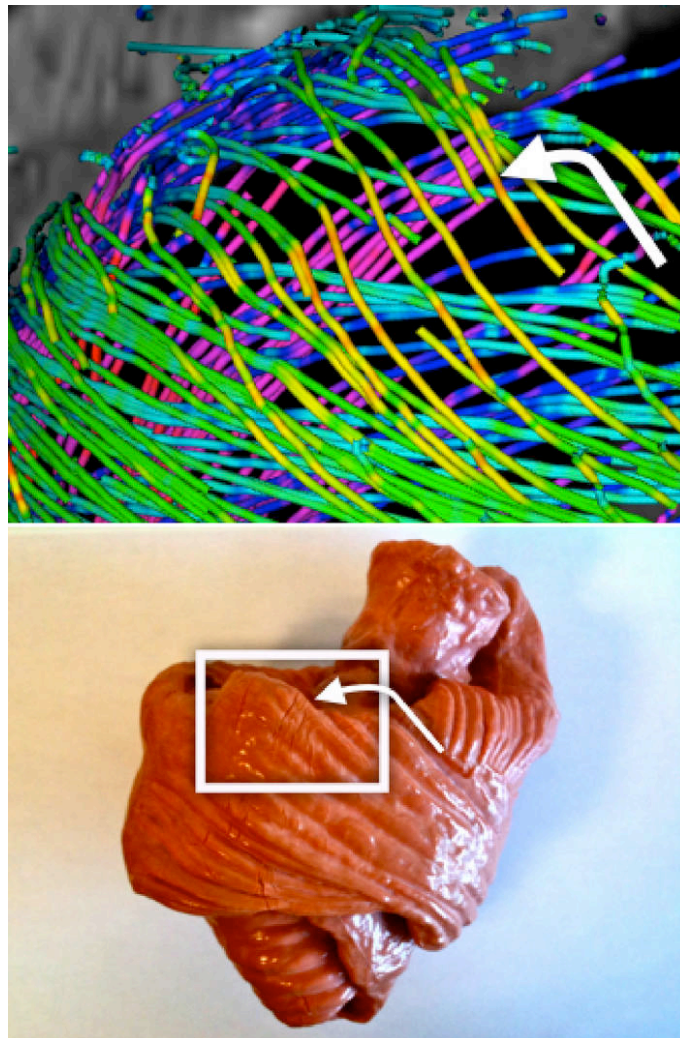


Figure 6: Comparison between DT-MRI tracts and a HVMB mould. Left segment, corresponding to the basal ring of the left ventricular myocardium.

As we track through lower streamlines, these lines are organized more horizontally but preserving a slight slope. We can see that these lines describe trajectories that wrap around the left ventricle connecting to further folds at the basal ring (Fig. 7).

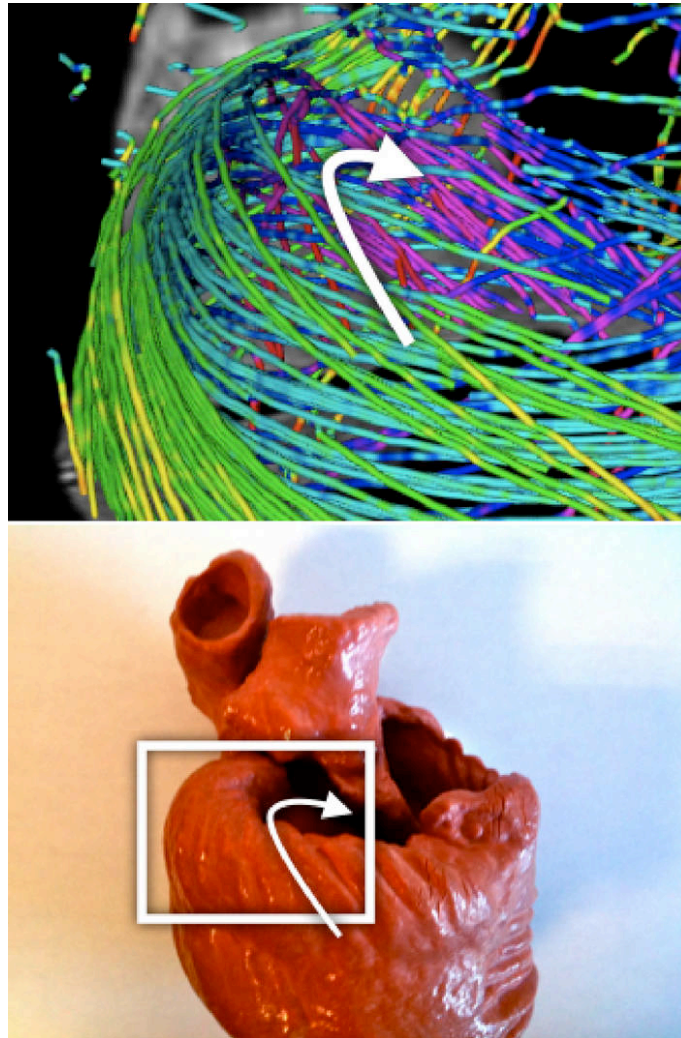


Figure 7: Comparison between diffusion tensor magnetic resonance imaging tracts and a helical ventricular myocardial band mould. Left segment, corresponding to the basal ring of the left ventricular myocardium

6.1.2. *Left Segment*

the previous pattern is reproduced along the left segment. At the end of this segment we can notice that the mentioned folding ends at the point where the streams get into the endocardium (Fig. 7).

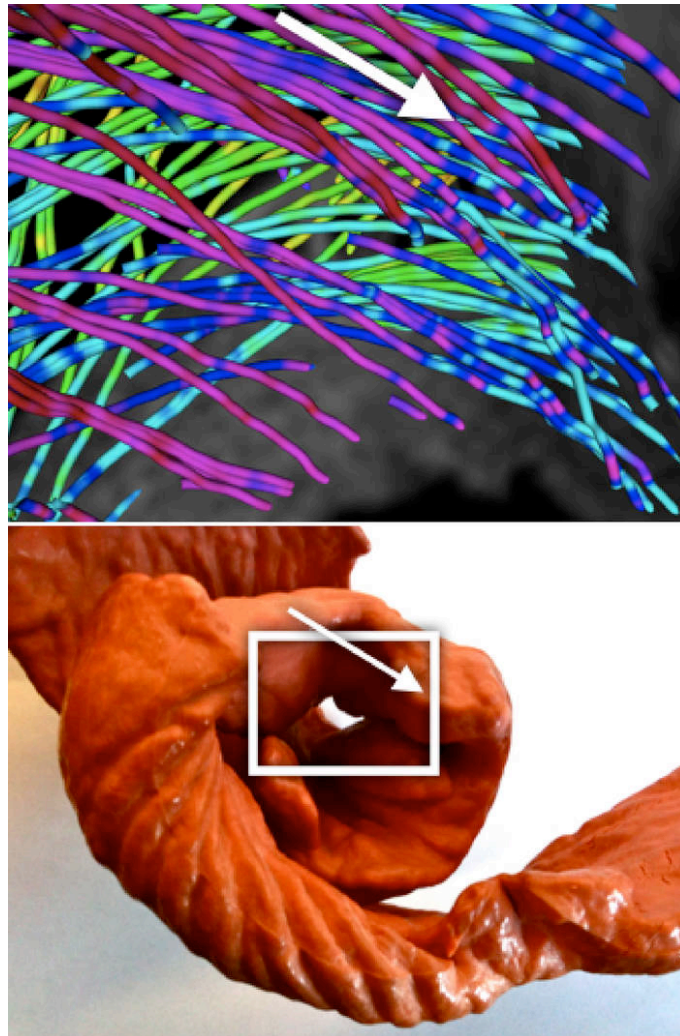


Figure 8: Comparison between diffusion tensor magnetic resonance imaging tracts and a helical ventricular myocardial band mould. Descending segment, corresponding to the inner wall of the left ventricular myocardium.

Descending Segment: from an anterior view (Fig. 8) we can clearly distinguish a spiral-descending organization of the endocardium population of streams across the septum. This structure continues to the apex and most of these streams continue on the right segment. Behind this endocardial structure it is also easy to notice an ascending structure that we will analyze in the following section from another visualization point of view.

6.1.3. Ascending Segment

The analysis of this segment is more complex due the cluttered view of several crossings of myocyte populations. With less streamlines than on the previous captures, figure 9 can show 3 populations where we can see that in this area streams coming from the apex start a noticeable ascend (fading from green to red coloration of the streams denoting an increase of the slope of this streams) below the two other populations that are the beginning of the right segment on its connection with the pulmonary artery.

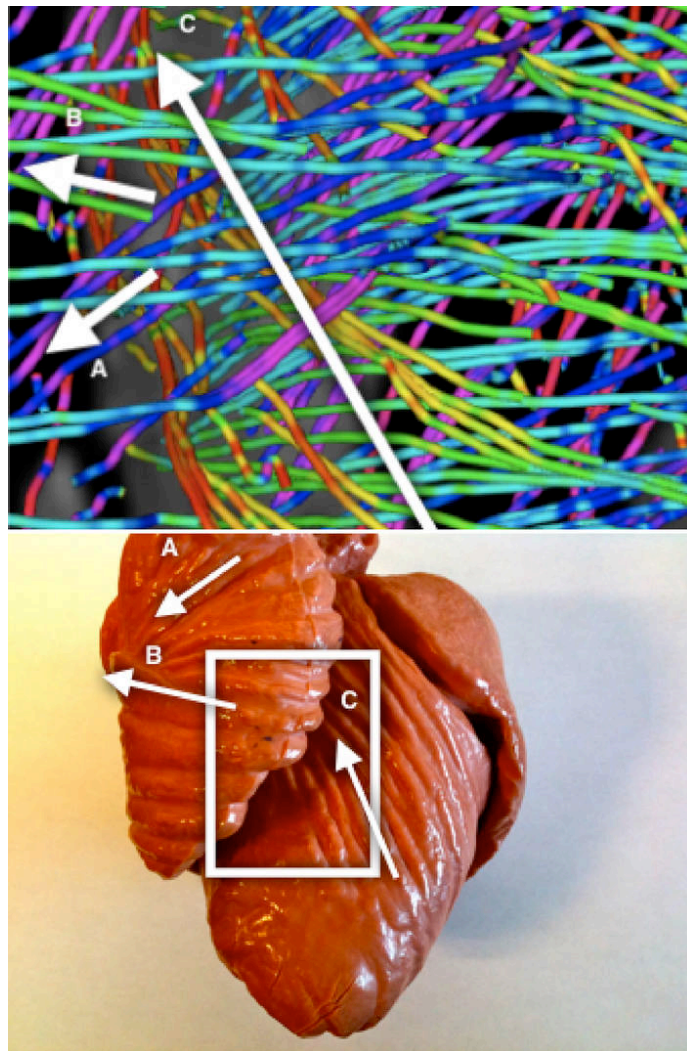


Figure 9: Comparison between diffusion tensor magnetic resonance imaging tracts and a helical ventricular myocardial band mould. Ascending segment, corresponding to the outer wall of the left ventricular myocardium.

6.2. Simplified Tractography

Although our simplified models provide easier interpretation of global tendencies, they are still too complex for summarizing complex structure such as the Torrent-Guasp's HVMB.

In order to simplify the backbone myocardial fiber spatial orientation we have explored the geometry of the heart by looking for long paths that can represent connected regions on the DTMRI tractography. The goal of this procedure was to provide a comprehensive reconstruction allowing interpretation at first sight by any possible observer.

By manually picking seeds at the basal level we have obtained continuous paths connecting both ventricles and wrapping the whole myocardium. Figure 10 shows four tracts of simplified models reconstructed from manually picked seeds located at basal level near the pulmonary artery. We observe that the tracts define a sample-wide coherent helical structure for all canine samples.

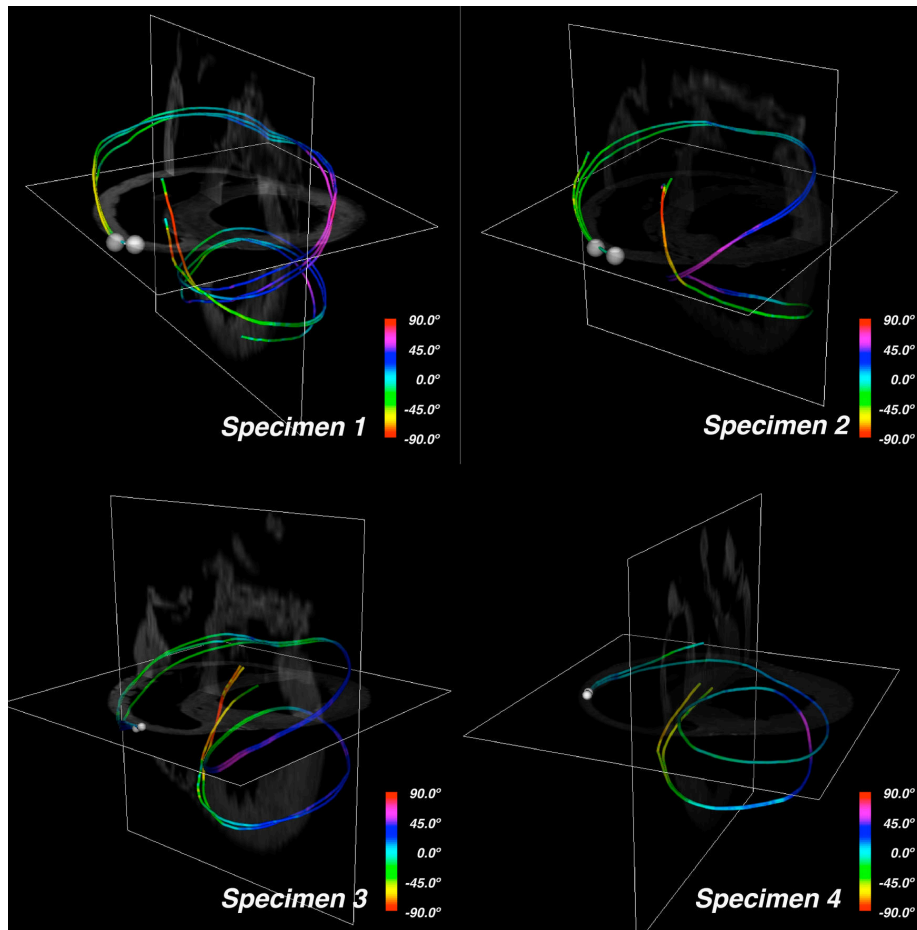


Figure 10: Simplified ventricular tractographies. Example of tracts reconstructed with manually picked seeds (always chosen near the pulmonary artery) on simplified tractographies

The use of visualizations with single tracts changes the way in which this structure can be viewed. We have compared such tracts to the proposed HVMB (Fig. 11). There is a clear similarity between the HVMB schematic model (Fig. 11, left) and reconstructed paths (Fig. 11, right). In both models the main segments (labeled from A to G) of the helical architecture are clearly identified.

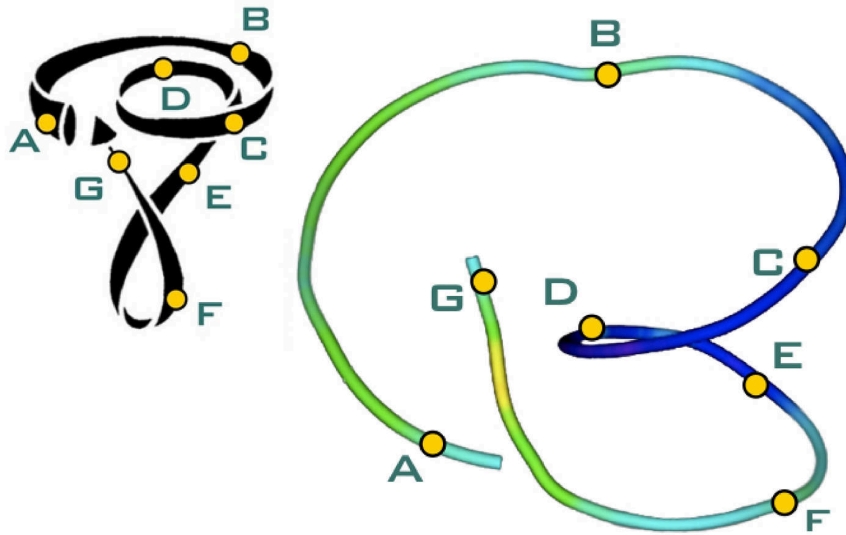


Figure 11: Comparison between helical ventricular myocardial band scheme and a simplified ventricular tractography. Torrent-Guasp’s helical ventricular myocardial band model compared to a tract reconstructed from a single manually picked seed on the diffusion tensor magnetic resonance imaging volume with landmarks for comparison with the model.

7. Discussion

The present paper provides an objective interpretation of the myocardial architecture based on automated descriptions of DT-MRI. Results show an unequivocal ventricular fiber connectivity describing a continuous muscular structure constituting the two ventricles arranged in a double helical orientation. This supports Torrent-Guasp’s description of the HVMB. These results are shown by unique automatically generated tracts that describe this connectivity along the whole myocytal mesh starting at the pulmonary artery and finishing at the aorta.

DT-MRI provides worthy and detailed information of myocardial tissue. However, interpretation of its outcome for heart architecture validation is not direct. Existing techniques reconstruct full heart anatomy using visual cues. Since tractography was proposed and used for the first time for heart structure study [23, 33], it has been the most common technique to recover information from DT-MRI. Other techniques have

been also explored as those in the work of Frindel [25] based on the optimization of graph models which promise future developments.

There are many factors that should be taken into account in order to obtain widely acceptable reconstructions and interpretations. It follows that most of the existing approaches [23, 24, 25, 26, 34, 35] do not provide enough evidence widely accepted by the whole scientific community for either supporting or invalidating any particular architectural model. The only agreement is the existence of a layered structure of the myocardium through tractographic representations and visualization improvements in color coding. Among these works, we want to remark the work of Helm [26] since, by its level of detail, it has been widely discussed on the literature hinting opposite readings. Such disagreement is direct consequence of a partial reconstruction of heart fiber anatomy.

In order to settle this disagreement we have used all the data in DT-MRI without segmentation to avoid instrumentalization of the study, and we have demonstrated that it is possible to reconstruct the whole myocardium including some complex structures as the basal loop, unfortunately hidden or misinterpreted by other studies. For this it has been also necessary to define a method to ensure a correct use of streamlining techniques to the particularities of the DT-MRI vector fields.

Validation of the correctness of local structures is not enough to extend the interpretation to a global point of view. Hence, to deal with higher level interpretations of the architectural organization of the heart we have also looked for higher level representations that can ease its interpretation and validation. We have contributed a multi-resolution method for tractography which using downsampling of the DT-MRI volumes can show global features of the heart structure. This work also includes colouring techniques applied to our solution which can ease the reading of the tractographic 3D models.

For studies requiring Q-ball analysis it is mandatory to use not less than 60 directions per voxel. However, DTI tensors only provide an average description of water diffusion and, thus, a large number of diffusion directions do not significantly improve their quality. It follows that existing DTI cardiac studies (like the widespread used JHU data set [36]) for DTI tensor analysis usually restrict values between 12 and 32 directions [37] for the sake of a good compromise between acquisition time and quality. Furthermore, a recent study reports that DTI primary eigenvector is invariant under a large variation of acquisition device parameters and, in particular, to a low number of diffusion directions [38]. Our own research suggests that heart preparation and volume spatial resolution are, indeed, one of the most influencing conditions on DTI quality. Acquisition field-of-view should be carefully adjusted to fit just the myocardial volume, which should be in suspension inside a recipient in order to avoid distortions in diffusion near myocardial boundaries.

We are currently acquiring our dataset from pig hearts using a 3T Philips device with 32 gradients, a volume resolution of $1.38 \times 1.38 \times 1.5$ micres ($144 \times 144 \times 60$ voxels) covering a heart short axis ROI of 70×70 pixels. Figure 12 shows a full resolution tractographic reconstruction of muscular fibers obtained using our software. The colouring indicates the sign of the fiber z-component (red for positive and green for negative) and, thus, its orientation. The transition fiber loop from epicardium to endocardium is clearly seen in the left lateral segment of the left ventricular base. We observe that the conclusions derived in this paper keep valid on this higher quality DT-MRI heart study.

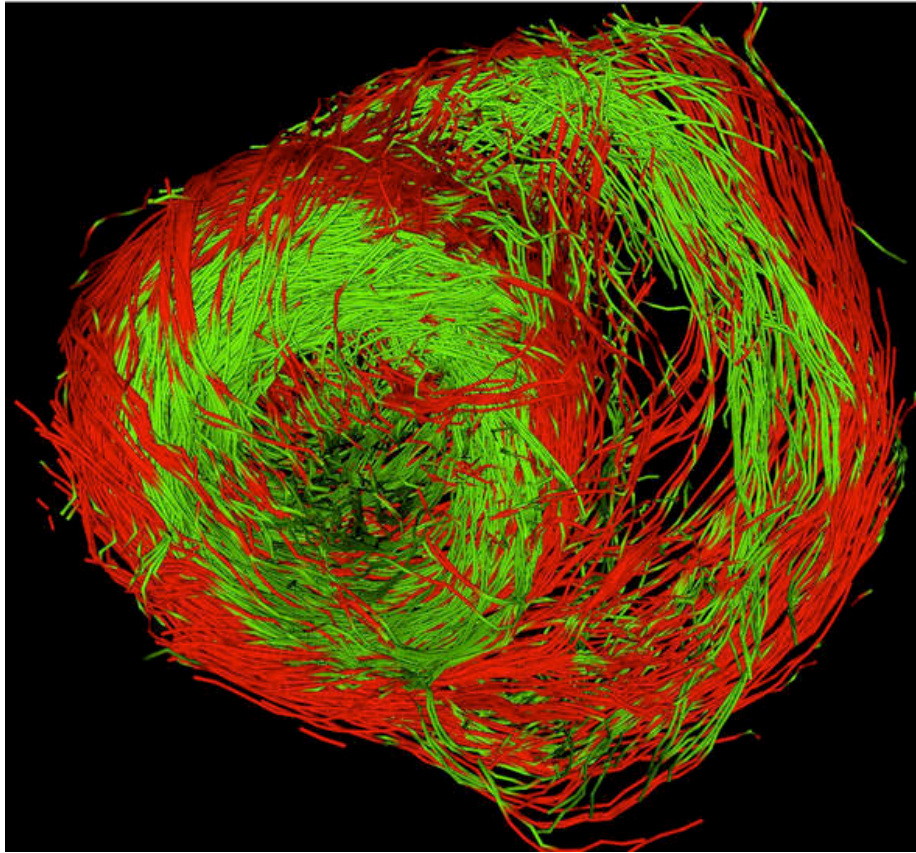


Figure 12: High resolution reconstruction of a diffusion tensor magnetic resonance imaging from a pig heart obtained with a 3T magnet (see text).

8. Conclusions

The objective analysis of myocardial architecture by an automated method including the entire myocardium and using several 3D levels of complexity reveals a continuous helical myocardial fiber arrangement of both right and left ventricles, thus supporting the anatomical studies performed by F. Torrent-Guasp.

9. Acknowledgements

We want to acknowledge Drs. Patrick A. Helm and Raimond L. Winslow at the Center for Cardiovascular Bioinformatics and Modeling and Dr. Elliot McVeigh at the National Institute of Health for provision of datasets of DT-MRI. This work was supported by the Spanish TIN2009-13618 and TIN2012-33116.

References

1. Roberts, D.E., Hersh, L.T., Scher, A.M.. Influence of cardiac fiber orientation on wavefront voltage, conduction velocity, and tissue resistivity in the dog. *Circ Res* 1979;**44**(5):701--12.
2. Taccardi, B., Punske, B.B., Macchi, E., Macleod, R.S., Ershler, P.R.. Epicardial and intramural excitation during ventricular pacing: effect of myocardial structure. *Am J Physiol Heart Circ Physiol* 2008;**294**(4):H1753--66. doi:10.1152/ajpheart.01400.2007.
3. LeGrice, I.J., Takayama, Y., Covell, J.W.. Transverse shear along myocardial cleavage planes provides a mechanism for normal systolic wall thickening. *Circ Res* 1995;**77**(1):182--93.
4. Zoalo Y Guevara E, B.D.e.a.. La reducción en el nivel y la velocidad de la torsión ventricular puede asociarse a incremento en la eficiencia ventricular izquierda: evaluación mediante ecografía speckle-tracking. *Rev Esp Cardiología* 2008; **61**:705--713.
5. Roberts, W.C., Siegel, R.J., McManus, B.M.. Idiopathic dilated cardiomyopathy: analysis of 152 necropsy patients. *Am J Cardiol* 1987;**60**(16):1340--55.
6. Wickline, S.A., Verdonk, E.D., Wong, A.K., Shepard, R.K., Miller, J.G.. Structural remodeling of human myocardial tissue after infarction. quantification with ultrasonic backscatter. *Circulation* 1992;**85**(1):259--68.
7. Ballester M Ferreira A, C.F.. The myocardial band. *Heart Fail Clin* 2008;**4**:261--272. doi:10.1016/j.hfc.2008.02.011.
8. Aguilar, J.A.C., Martínez, A.H., Segarra, M.T.T., Ramón-Llin, J.A., Torrent-Guasp, F.. Estudio experimental de la llamada fase de relajación isovolumétrica del ventrículo izquierdo. *Revista Espanola De Cardiologia* 2009;**62**:392--399. doi:10.1016/S0300-8932(09)70896-6.
9. Torrent Guasp, F., JM, C.R., Ballester Rodés, M.. Cuatro propuestas para la remodelación ventricular en el tratamiento de la miocardiopatía dilatada. *Rev Esp Cardiología* 1997;**50**:682--690.
10. Jung, B.A., Kreher, B.W., Markl, M., Hennig, J.. Visualization of tissue velocity data from cardiac wall motion measurements with myocardial fiber tracking: principles and implications for cardiac fiber structures. *Eur J Cardiothorac Surg* 2006;**29 Suppl 1**:S158--64. doi:10.1016/j.ejcts.2006.02.060.
11. Gilbert, S.H., Benson, A.P., Li, P., Holden, A.V.. Regional localisation of left ventricular sheet structure: integration with current models of cardiac fibre, sheet and band structure. *European Journal of Cardio-Thoracic Surgery* 2007;**32**(2):231--249. URL: <http://ejcts.oxfordjournals.org/content/32/2/231.abstract>. doi:10.1016/j.ejcts.2007.03.032. arXiv:<http://ejcts.oxfordjournals.org/content/32/2/231.full.pdf+html>.

12. Anderson, R.H., Ho, S.Y., Redmann, K., Sanchez-Quintana, D., Lunkenheimer, P.P.. The anatomical arrangement of the myocardial cells making up the ventricular mass. *Eur J Cardiothorac Surg* 2005;**28**(4):517--25. doi:10.1016/j.ejcts.2005.06.043.
13. Anderson, R.H., Smerup, M., Sanchez-Quintana, D., Loukas, M., Lunkenheimer, P.P.. The three-dimensional arrangement of the myocytes in the ventricular walls. *Clin Anat* 2009;**22**(1):64--76. doi:10.1002/ca.20645.
14. F, T.G.. Estructura y función del corazón. *Rev Esp Cardiol* 1985;**51**:91--102.
15. Torrent Guasp, F., Ballester, M., Buckberg, G.D., Carreras, F., Flotats, A., Carrió, I., et al. Spatial orientation of the ventricular muscle band: physiologic contribution and surgical implications. *J Thorac Cardiovasc Surg* 2001;**122**(2):389--92. doi:10.1067/mtc.2001.113745.
16. Torrent Guasp, F.. La mecánica agonista-antagonista de los segmentos descendente y ascendente de la banda miocárdica ventricular. *Rev Esp Cardiología* 2001; **54**:1091--102.
17. Carreras, F., Garcia-Barnes, J., Gil, D., Pujadas, S., Li, C.H., Suarez-Arias, R., et al. Left ventricular torsion and longitudinal shortening: two fundamental components of myocardial mechanics assessed by tagged cine-mri in normal subjects. *Int J Cardiovasc Imaging* 2012;**28**(2):273--84. doi:10.1007/s10554-011-9813-6.
18. LeGrice, I.J., Smail, B.H., Chai, L.Z., Edgar, S.G., Gavin, J.B., Hunter, P.J.. Laminar structure of the heart: ventricular myocyte arrangement and connective tissue architecture in the dog. *Am J Physiol* 1995;**269**(2 Pt 2):H571--82.
19. Scollan, D.F., Holmes, A., Winslow, R., Forder, J.. Histological validation of myocardial microstructure obtained from diffusion tensor magnetic resonance imaging. *Am J Physiol* 1998;**275**(6 Pt 2):H2308--18.
20. de Figueiredo, E.H.M.S.G., Borgonovi, A.F.N.G., Doring, T.M.. Basic concepts of mr imaging, diffusion mr imaging, and diffusion tensor imaging. *Magn Reson Imaging Clin N Am* 2011;**19**(1):1--22. doi:10.1016/j.mric.2010.10.005.
21. Poveda, F., Martí, E., Gil, D., Carreras, F., Ballester, M.. Helical structure of ventricular anatomy by diffusion tensor cardiac mr tractography. *JACC Cardiovasc Imaging* 2012;**5**(7):754--5. doi:10.1016/j.jcmg.2012.04.005.
22. University, J.H.. Public dt-mri dataset. 2011. URL: http://gforge.icm.jhu.edu/gf/project/dtmri_data_sets/.
23. Zhukov, L., Barr, A.H.. Heart-muscle fiber reconstruction from diffusion tensor mri. In: *Proc. IEEE Visualization Conf.* 2003, p. 79.

24. Rohmer, D., Sitek, A., Gullberg, G.T.. Reconstruction and visualization of fiber and laminar structure in the normal human heart from ex vivo diffusion tensor magnetic resonance imaging (dtmri) data. *Invest Radiol* 2007;**42**(11):777--89. doi:10.1097/RLI.0b013e3181238330.
25. Frindel, C., Schaerer, J., Gueth, P., Clarysse, P., Zhu, Y.M., Robini, M.. A global approach to cardiac tractography. In: *Biomedical Imaging: From Nano to Macro, 2008. ISBI 2008. 5th IEEE International Symposium on*. 2008, p. 883--886. doi:10.1109/ISBI.2008.4541138.
26. Helm, P., Beg, M.F., Miller, M.I., Winslow, R.L.. Measuring and mapping cardiac fiber and laminar architecture using diffusion tensor mr imaging. *Ann N Y Acad Sci* 2005;**1047**:296--307. doi:10.1196/annals.1341.026.
27. Gil, D., Garcia-Barnes, J., Hernández-Sabate, A., Marti, E.. Manifold parametrization of the left ventricle for a statistical modelling of its complete anatomy. In: *Society of Photo-Optical Instrumentation Engineers (SPIE) Conference Series*; vol. 7623 of *Society of Photo-Optical Instrumentation Engineers (SPIE) Conference Series*. 2010, doi:10.1117/12.844480.
28. Granger, R.. *Fluid mechanics*. Mineola, NY: Courier Dover Publications; 1995.
29. Fehlberg, E.. Klassische runge-kutta-formeln vierter und niedrigerer ordnung mit schrittweiten-kontrolle und ihre anwendung auf wärmeleitungsprobleme. *Computing (Arch Elektron Rechnen)* 1970;**6**:61--71.
30. Williams, L.. Pyramidal parametrics. *SIGGRAPH Comput Graph* 1983;**17**(3):1-11. URL: <http://doi.acm.org/10.1145/964967.801126>. doi:10.1145/964967.801126.
31. Burt, P.J.. Fast filter transform for image processing. *Graphical Models /graphical Models and Image Processing /computer Vision, Graphics, and Image Processing* 1981;**16**:20--51. doi:10.1016/0146-664X(81)90092-7.
32. Torrent Guasp, F., Whimster, W.F., Redmann, K.. A silicone rubber mould of the heart. *Technol Health Care* 1997;**5**(1-2):13--20.
33. Basser, P.J., Pajevic, S., Pierpaoli, C., Duda, J., Aldroubi, A.. In vivo fiber tractography using dt-mri data. *Magn Reson Med* 2000;**44**(4):625--32.
34. Schmid, P., Jaermann, T., Boesiger, P., Niederer, P.F., Lunkenheimer, P.P., Cryer, C.W., et al. Ventricular myocardial architecture as visualised in post-mortem swine hearts using magnetic resonance diffusion tensor imaging. *Eur J Cardiothorac Surg* 2005;**27**(3):468--72. doi:10.1016/j.ejcts.2004.11.036.
35. Peeters, T., Bartroli, A.V., Strijkers, G., ter Haar Romeny, B.. Visualization of the fibrous structure of the heart. In: *VMV 2006*. 2006, p. 309--316.

36. Sermesant, M., Chabiniok, R., Chinchapatnam, P., Mansi, T., Billet, F., Moireau, P., et al. Patient-specific electromechanical models of the heart for the prediction of pacing acute effects in crt: a preliminary clinical validation. *Med Image Anal* 2012;**16**(1):201--15. doi:10.1016/j.media.2011.07.003.
37. Krishnamurthy, A., Villongco, C.T., Chuang, J., Frank, L.R., Nigam, V., Belezouli, E., et al. Patient-specific models of cardiac biomechanics. *Journal of Computational Physics* 2012;(0):-- . URL: <http://www.sciencedirect.com/science/article/pii/S0021999112005463>. doi:10.1016/j.jcp.2012.09.015.
38. Gilbert, S., Trew, M., Smaill, B., Radjenovic, A., Bernus, O.. Measurement of myocardial structure: 3d structure tensor analysis of high resolution mri quantitatively compared to dt-mri. In: Camara, O., Mansi, T., Pop, M., Rhode, K., Sermesant, M., Young, A., editors. *Statistical Atlases and Computational Models of the Heart. Imaging and Modelling Challenges*; vol. 7746 of *Lecture Notes in Computer Science*. Springer Berlin Heidelberg. ISBN 978-3-642-36960-5; 2013, p. 207--214. URL: http://dx.doi.org/10.1007/978-3-642-36961-2_24. doi:10.1007/978-3-642-36961-2_24.